Technical note: In situ U–Th–He dating by [4]He/[3]He laser microprobe analysis

Pieter Vermeesch[1], Yuntao Tian[1,2], Jae Schwanethal[1], and Yannick Buret[3]

[1]London Geochronology Centre, Department of Earth Sciences, University College London, Gower Street, London WC1E 6BT, United Kingdom
[2]Guangdong Provincial Key Laboratory of Geodynamics and Geohazards, School of Earth Sciences and Engineering, Sun Yat-sen University, Guangzhou 510275, China
[3]Department of Earth Sciences, Natural History Museum, Cromwell Road, London SW7 5BD, United Kingdom

Correspondence: Pieter Vermeesch (p.vermeesch@ucl.ac.uk)

Abstract. In-situ U-Th-He geochronology is a potentially disruptive technique that combines laser ablation inductively coupled plasma mass spectrometry with laser microprobe noble gas mass spectrometry. Despite its potential to revolutionise (detrital) thermochronology, in-situ U-Th-He dating is not widely used, due to persistent analytical challenges. The main issue is that currently used approaches to in-situ dating require that the U, Th and He measurements are expressed in units of molar
5 concentration, in contrast with conventional methods, which use units of molar abundance. Whereas molar abundances can be reliably determined by isotope dilution, accurate concentration measurements are not so easy to obtain. In the absence of matrix-matched U,Th-concentration standards and accurate He-ablation pit measurements, the accuracy of in-situ U-Th-He dates often leaves much to be desired. This paper proposes a solution to this problem, by using proton-induced [3]He as a proxy for ablation pit volume, and by pairing samples with a standard of known U-Th-He age. Thus, the U-Th-He age equation can be
10 solved using relative rather than absolute concentration measurements. Pilot experiments show that the new method produces accurate results. However, it is prone to overdispersion, which is attributed to gradients in the proton fluence. These gradients can be measured and their effect can be removed by fixing the geometry of the sample and the standard during the proton irradiation.

1 Introduction

15 Conventional U-Th-He thermochronology is labour intensive, especially for zircon. It involves (1) identifying suitable crystals under a binocular microscope; (2) measuring their three-dimensional size to estimate the fraction of helium lost through α-ejection (Farley et al., 1996; Ketcham et al., 2011); (3) packing the individual crystals into Pt or Nd 'microfurnaces' (House et al., 2000); (4) degassing the crystals with a laser in ultrahigh vacuum and analysing the released gas by noble gas mass spectrometry; (5) recovering the degassed grains from the microfurnaces and dissolving them in hydrofluoric acid with a Parr
20 vessel; and (6) determining their U and Th content by isotope dilution ICP-MS (Figure 1A).

In-situ U-Th-He laser microprobe analysis simplifies or removes steps 2–6 of this procedure, which increases sample throughput whilst potentially improving accuracy as well (Boyce et al., 2006, 2009; Vermeesch et al., 2012; Tripathy-Lang

et al., 2013; Evans et al., 2015; Danišík et al., 2017). Furthermore, in-situ analysis of zircon essentially produces U-Pb double-dates as a byproduct, which opens new research opportunities in detrital geochronology. However, despite its appeal, the method has still not been widely adopted by thermochronologists nearly two decades after its initial development by Boyce et al. (2006). The slow uptake of in-situ U-Th-He dating has several causes, one of which is accuracy.

Measuring helium concentration (in units of atoms per unit volume) requires accurate estimates of ablation pit volume. Unfortunately, laser ablation produces irregularly shaped ablation pits in ultra-high vacuum conditions, making pit volume measurements difficult at best and inaccurate worst. Furthermore, the accuracy of the U and Th concentration measurements cannot be guaranteed either, due to the lack of matrix-matched concentration standards.

Vermeesch et al. (2012) proposed a simplified workflow that pairs the sample with a well characterised reference material of known U-Th-He age, thereby removing the need for accurate U and Th concentration measurements. Evans et al. (2015) reformulated this 'pairwise dating' approach in terms of a κ-calibration factor. Given the U/Si, Th/Si and He/V ratio measurements of a standard of known age t, where V is the ablation pit volume, the U-Th-He age equation can be written as:

$$\kappa \left[\frac{He}{V}\right] = \left\{8\frac{137.82}{138.82}\left(e^{\lambda_{38}t}-1\right) + \frac{7}{138.82}\left(e^{\lambda_{35}t}-1\right)\right\}\left[\frac{U}{Si}\right] + 6\left(e^{\lambda_{32}t}-1\right)\left[\frac{Th}{Si}\right] \tag{1}$$

where κ serves a similar purpose as the J-factor in ^{40}Ar/^{39}Ar geochronology (Merrihue and Turner, 1966) or the ζ-calibration factor in fission track thermochronology (Hurford and Green, 1983).

Although this method solves many of the practical difficulties of in-situ U-Th-He measurements, the need for ablation pit measurements remains. In its simplest form, the κ-calibration approach assumes that the drill rate of the UV laser is the same for the sample and the standard. Interferometric pit depth measurements indicate that this is not the case. For example, Vermeesch et al. (2012) observed drill rate differences of 15% even when identical laser settings were used to analyse different Sri Lanka zircon megacrysts. These drill rate differences were found to be roughly proporational to the Si-sensitivity differences measured by laser ablation inductively coupled plasma mass spectrometry (LA-ICP-MS), suggesting that Si can be used as a 'drill rate proxy' for the helium measurements.

Using Si as a proxy for pit depth works reasonably well for the samples of Vermeesch et al. (2012), but is imprecise and only works when samples and standards are analysed in the same analytical session, using identical laser settings. This limits the technique's potential for depth profiling and mapping.

This paper presents a progress report for a different approach to pairwise U-Th-He dating, using proton-induced ^{3}He as a proxy for ablation pit volume (Figure 1A). When zircon is irradiated with high energy protons in a particle accelerator, spallation reactions on Zr, Si and O produce a small but measurable amount of ^{3}He (Shuster et al., 2004). If a sample and co-irradiated reference materials have experienced the same proton fluence, then Equation 1 can be replaced with:

$$\kappa \left[\frac{^4He}{^3He}\right] = \left\{8\frac{137.82}{138.82}\left(e^{\lambda_{38}t}-1\right) + \frac{7}{138.82}\left(e^{\lambda_{35}t}-1\right)\right\}\left[\frac{U}{Si}\right] + 6\left(e^{\lambda_{32}t}-1\right)\left[\frac{Th}{Si}\right] \tag{2}$$

The following sections summarise experimental tests of this simple idea. These experiments that were carried out between 2014 and 2016 using financial support from the UK's Natural Environment Research Council (NERC, see Acknowledgments).

55   The research funding ended, the research team was dissolved, and research priorities shifted, so that the results of our work were never published. With this technical note, we would like to encourage others to continue were we left off, using the lessons that we have learned.
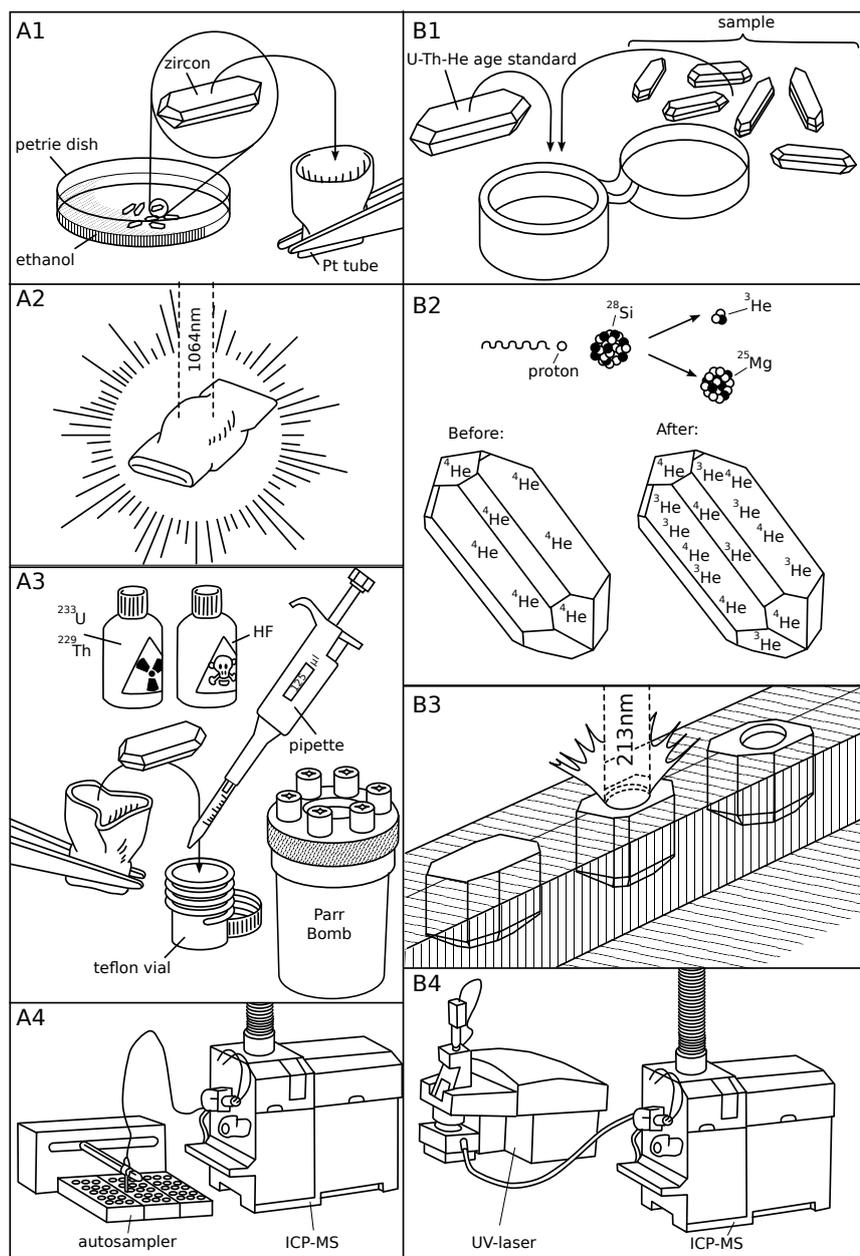
Figure 1. The analytical procedure for conventional U-Th-He dating (A) and the new in-situ ^{4}He/^{3}He laser microprobe method (B): A1. grain selection; A2. degassing by laser heating in a Pt microfurnace; A3. isotope dilution of U and Th; A4. U and Th analysis in solution; B1. packing sample and standard together; B2. proton irradiation; B3. ^{4}He/^{3}He analyses (of vertically mounted zircons) by UV laser microprobe noble gas mass spectrometry; B4. U and Th analysis by LA-ICP-MS.

2 Experimental designs

60 We tested three different experimental designs.

2.1 Loose grains

In a first set of experiments, loose grains of Fish Canyon zircon were packed together with Sri Lanka zircon LGC-1 (476.4±5.7 Ma, Tian et al., 2017). After proton irradiation, the grains were mounted in teflon, polished, and analysed for U, Th and He using procedures that are detailed in Section 3. These experiments produced generally accurate, but highly dis-

65 persed results (Figure 2). At first, we attributed this dispersion to compositional zoning of the Fish Canyon zircons (Figure 3): because helium is measured in a separate ablation spot than the U and Th, any difference in actinide concentration between the two spots causes inaccurate ages.
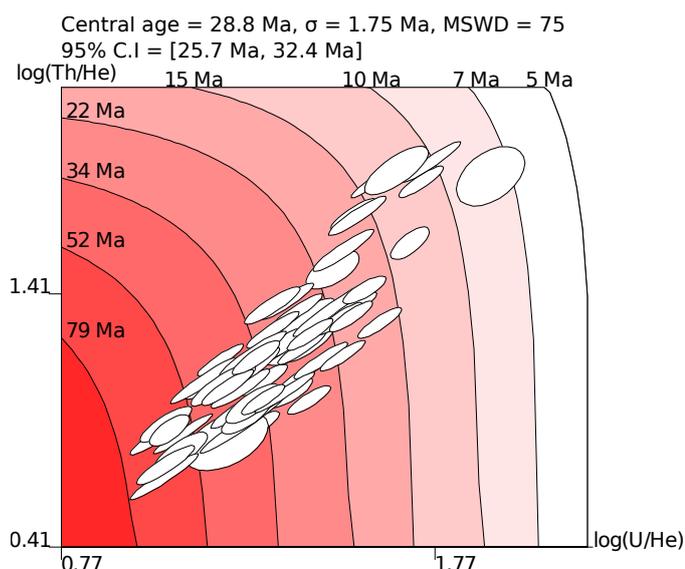
Figure 2. The U-Th-He compositions of 61 Fish Canyon zircons (white ellipses) follow a bivariate normal U-Th-He distribution in logratio space (Vermeesch, 2010). The mean composition corresponds to a U-Th-He age (the 'central age', Vermeesch, 2008) which is in excellent agreement with the known eruption age of the Fish Canyon Tuff (28.8Ma, Kuiper et al., 2008). The compositional MSDW of 75 indicates significant overdispersion with respect to the formal analytical precision, likely due to a combination of compositional zoning (Figure 3) and proton flux gradients.

2.2 Vertically mounted grains

70 Because compositional zoning tends to be largely concentric, we carried out some experiments using vertically mounted Fish Canyon zircons (Figure 3). This was achieved by (1) excavating a series of $100 \times 50 \times 50$ μm 'trenches' in sheets of teflon; (2) placing proton-irradiated zircons in them; (3) covering the grains with a second sheet of teflon; (4) welding the two sheets together by applying pressure to them on a hot plate at ca. 210°C; (5) polishing the edge of the resulting teflon 'sandwich'

75 until the apexes of the grains were removed; and (6) placing the teflon sheet upright in a bespoke sample holder. Helium was measured first, and after repolishing the U and Th were measured in a second ablation pit located down the c-axis from the first one. This elaborate procedure slightly reduced the dispersion, but unfortunately did not remove it.
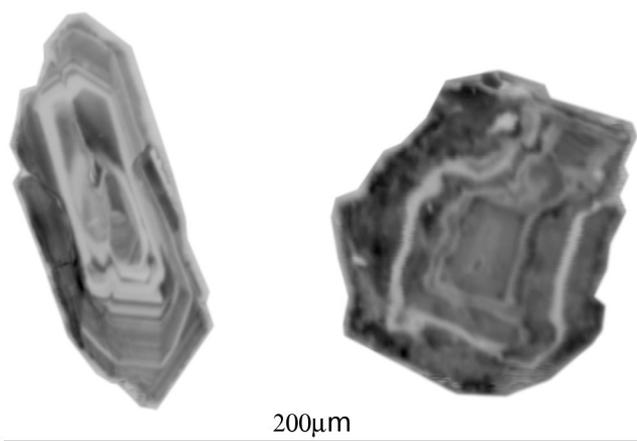
Figure 3. Cathodo-luminescence images of horizontally (left) and vertically (right) mounted Fish Canyon zircons, exhibiting predominantly c-axis concentric compositional zoning.

2.3 Sample-standard 'sandwiches'

The previous pair of experiments indicated that, although compositional zoning may be one factor degrading the accuracy of
80 in-situ U-Th-He dating, it is not the dominant factor. Closer inspection of the standards revealed marked differences in ^{4}He/^{3}He ratios within and between Sri Lanka megacryst shards. These differences suggest the presence of strong, mm-scale gradients in the proton fluence, despite the efforts taken to change the orientation of the samples during the irradiation.

To investigate this phenomenon and potentially fix it, we developed a third experimental design, in which the standard and sample are polished prior to irradiation and glued together along their polishing surfaces. This arrangement serves a dual
85 purpose. First, it ensures that each point in the sample receives exactly the same proton dose as its counterpart in the standard. Second, by attaching the sample to the standard, any spallogenic ^{3}He that passes through the polishing surface of the sample is injected into the standad and *vice versa*. This reduces potential geometric complications that may arise when comparing different sized crystals. We tested this approach using compositionally homogeneous GJ-1 (Jackson et al., 2004) as a sample, to avoid the confounding effect of textural complexity in FC zircon. The results of these experiments are described and discussed
90 in the remainder of this paper.

3 Analytical methods and data processing

The sample-standard sandwiches were packed together in HDPE vials (Posthumus Plastics capsule type H and snapcap type E) and proton-irradiated at the Harvard Cyclotron Center using procedures outlined by Shuster et al. (2004). Samples were attached to standards using super glue, and were detached after irradiation by dissolution of the glue with acetone in an ultrasonic bath. The detached crystals were rinsed in de-ionised water and mounted in indium. Photographically identified contact points were used to match any location in the sample with its 'mirror image' in the standard.

Helium was released from the zircon grains by ablation with a UP-213 frequency-quintupled Nd-YAG laser in a small (5 cm diameter) ablation cell with sapphire window. Typical spot sizes were 90 μm in diameter, with ablation occurring at 20 Hz for 30 seconds. ^{4}He was measured on a Faraday detector and ^{3}He on a secondary electron multiplier (SEM) in peaking hopping mode (using either six or twenty 85-second cycles) on a Nu Instruments Noblesse sector field noble gas mass spectrometer at University College London. The extraction line of this instrument is described by Schwanethal (2015), as is the procedure to minimise the ^{12}C^{3+} interference on ^{4}He.

The ^{4}He/^{3}He ratio was obtained by linear regression of the ^{4}He signals and ^{3}He to 'time zero', which corresponds to the time when the cleaned gas was introduced into the ionisation volume of the mass spectrometer. The resulting values have units of kV/Hz. Note that these units vanish from the age equation after encapsulation in the κ-calibration constant (Equation 1). Thus, our method does not require the sensitivity of the Faraday and SEM detectors to be inter-calibrated.

The U and Th content of the samples was analysed by LA-ICP-MS at the Natural History Museum, using an Agilent 8900 instrument that was coupled with a Teledyne Cetac Iridia laser. This setup is optimised for raster imaging applications. Each grain was mapped using a 10×10 μm square spot with an energy density of 2.5 J/cm^2, a repetition rate of 400 Hz and a scan speed of 400 μm/s. ICP-MS measurements used dwell times of 2.5 ms for all measured isotopes (^{29}Si, ^{206}Pb, ^{232}Th and ^{238}U). NIST SRM610 was used as a concentration standard and 91500 zircon as a secondary reference material. Data reduction was done with Teledyne Cetac's HDIP software. This method allowed us to create U,Th-maps with 10 μm horizontal resolution. These detailed maps allowed us to (1) detect any compositional zoning in the sample and standard, and (2) interpolate the U,Th-concentrations to the locations of the helium analysis spots.

This analytical protocol produces the following data files:

1. A table with the coordinates (x, y) of the helium ablation spots, the corresponding blank-corrected ^{4}He/^{3}He measurements, and their standard errors, for both halves of the sample-standard sandwich. The coordinates can be expressed in LA-ICP-MS laser stage coordinates by identifying the helium ablation spots in the U,Th-map.

2. Two grids of U and Th concentration measurements or, equivalently, U/Si and Th/Si ratio measurements.

3. A table of fiducial points, recording the positions of at least three matching locations in the sample and the standard, recorded in LA-ICP-MS laser stage coordinates.

Given these three pieces of information, the U-Th-He ages are calculated as follows:

1. Map the coordinates of the standard onto those of the sample by Procrustes analysis, using the fiducial points (Figure 4a-b).

125 2. Interpolate the U and Th concentration (or U/Si and Th/Si ratio) measurements to the locations of the ^{4}He/^{3}He measurements (Figure 4c).

3. Calculate the κ-calibration constant for each helium ablation spot in the standard, given its known age and U, Th and ^{4}He/^{3}He measurement.

4. Interpolate the κ-values of the standard to the locations of the helium measurements in the sample.

130 5. Combine the κ parameter with the ^{4}He/^{3}He, U and Th measurements of the sample to calculate the U-Th-He age (Figure 4.d-e).

4   Results

Inspection of the analytical results for two standard-sample pairs (Tables 1 and 2) reveals a number of patterns. First, the ^{4}He/^{3}He ratios vary significantly between different shards of LGC-1 and GJ-1. They are, on average, 25% higher for the first

135 pair than for the second pair. In contrast, the U and Th concentrations of the two pairs of shards are nearly identical. This discrepancy between the two sets of measurements can only have one cause, namely the presence of significant gradients in the proton fluence received by different parts of the 'rabbit'. These gradients are reflected in the κ-values, which vary in tandem with the ^{4}He/^{3}He measurements.

Whilst the κ-values vary by a factor of two between the pairs, smaller gradients are visible within them. For example, pair 1

140 exhibits a ~15% difference in κ-values over a distance of ~500 µm. Fitting an interpolation surface to these values undoes the effect of the proton gradient and produces more accurate ages (Figure 4.c).

For pair 1, the in-situ U-Th-He ages range from 420 to 520 Ma, with a central age of 453±8 Ma, which is in good agreement with conventional U-Th-He ages of GJ-1 (456±13 Ma, Table 3). The second pair yields equally accurate ages, ranging from 420 to 500 Ma with a central value of 457±24 Ma. The compositional MSWDs (as defined by Vermeesch, 2010) of 1.5 for the

145 first pair (Figure 4e), and 2.3 for the second pair indicate that overdispersion is minor. Thus, the sandwich technique appears to have successfully removed the proton fluence gradient.
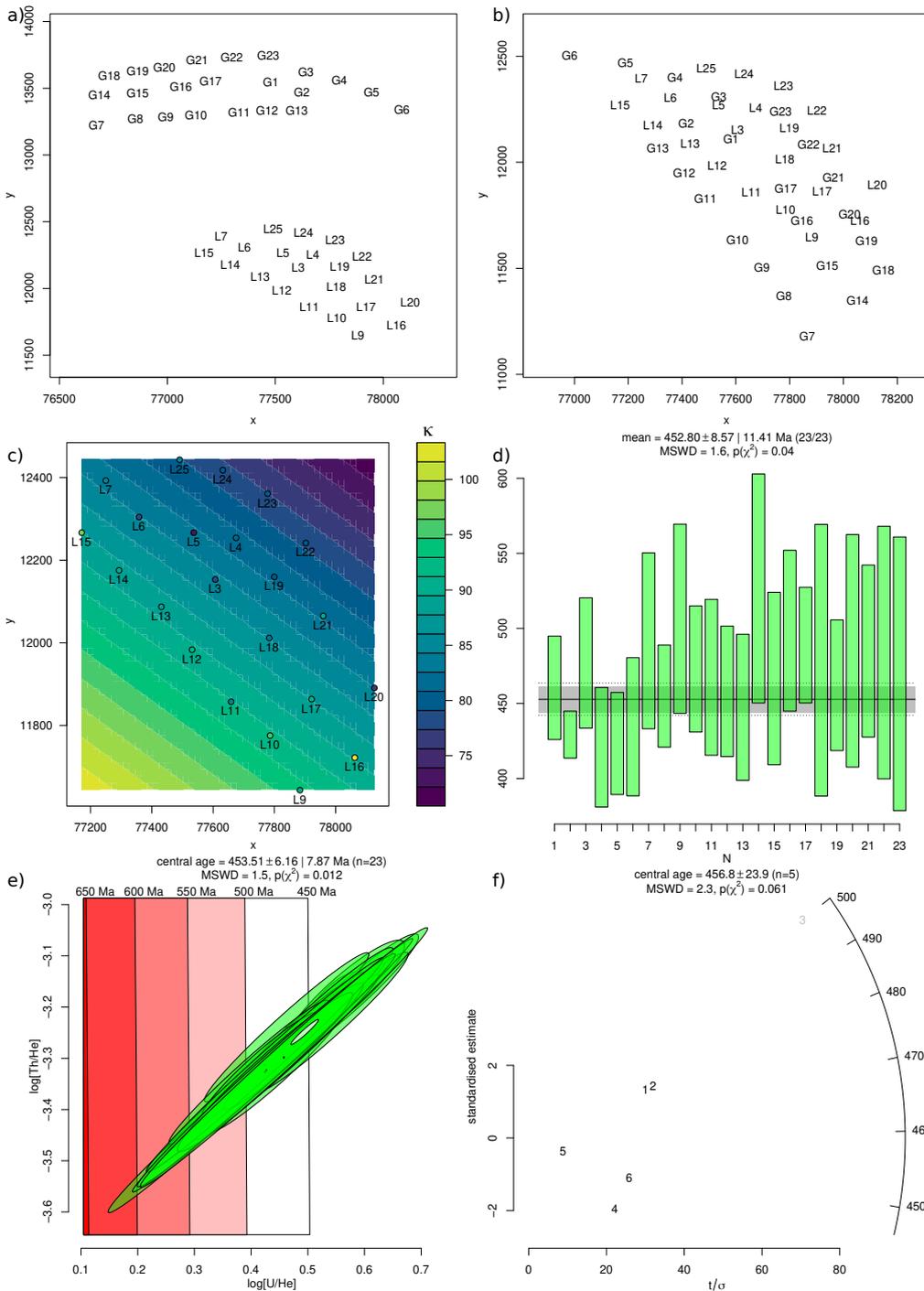
Figure 4. a) stage coordinates of the helium measurements for the standard ('L' is short for 'LGC-1') and sample ('G' is short for 'GJ-1') of the first sample-standard pair; b) Procrustes-transformation of the coordinates in the previous panel; c) linear interpolation surface of the κ-values for LGC-1; d) U-Th-He age estimates for the first sample-standard pair with the conventional age (456.0 ± 12.7 Ma) marked

by a dashed line; e) U-Th-He compositions for the first sample-standard pair; f) radial plot with the U-Th-He age estimates for the second sample-standard pair, with the third aliquot omitted as an outlier.

Table 1. Analytical results for the first pair of LGC-1 and GJ-1 shards. Row names represent helium laser ablation spots (LGC1-1-n and GJ1-1-n where 'n' is a number) and fiducial marks (LGC1-1-X and GJ1-1-X where 'X' is a letter). Columns x and y represent the raw LA-ICP-MS stage coordinates (in microns) of the helium spots; x' and y' are the coordinates after Procrustes transformation; ^{4}He/^{3}He and s[^{4}He/^{3}He] have units of kV/Hz; ^{3}He has units of Hz; U, s[U], Th and s[Th] have units of ppm; κ and s[κ] have units of Hz/kV; and t and s[t] are in Ma.

	x	y	x'	y'	^{4}He/^{3}He	s[^{4}He/^{3}He]	^{3}He	U	s[U]	Th	s[Th]	κ	s[κ]	t	s[t]
LGC1-1-A	77776	12719													
LGC1-1-B	78317	11724													
LGC1-1-C	76709	12592													
LGC1-1-3	77606	12155	77606	12155	3.59	0.118	12	310	2	570	3.5	77.9	2.61	476.4	5.7
LGC1-1-4	77674	12256	77674	12256	3.42	0.224	21	310	2	570	3.8	82.2	5.41	476.4	5.7
LGC1-1-5	77536	12268	77536	12268	3.83	0.0908	18	310	2.2	570	3.7	73.5	1.82	476.4	5.7
LGC1-1-6	77357	12306	77357	12306	3.58	0.213	21	310	2.1	570	3.6	78.4	4.68	476.4	5.7
LGC1-1-7	77249	12394	77249	12394	3.37	0.0965	22	310	1.8	570	3.2	84.5	2.46	476.4	5.7
LGC1-1-9	77883	11645	77883	11645	3.25	0.125	21	320	2	600	4	89.9	3.52	476.4	5.7
LGC1-1-10	77785	11777	77785	11777	3.05	0.129	13	320	2	590	4.4	95.4	4.09	476.4	5.7
LGC1-1-11	77658	11859	77658	11859	3.4	0.189	12	310	1.9	590	3.9	84.5	4.73	476.4	5.7
LGC1-1-12	77530	11985	77530	11985	3.06	0.0805	13	310	2.1	580	3.9	91.8	2.5	476.4	5.7
LGC1-1-13	77430	12089	77430	12089	3.17	0.154	13	310	2.3	570	4	88.8	4.36	476.4	5.7
LGC1-1-14	77292	12177	77292	12177	3.12	0.0641	13	310	1.9	580	3.3	90.9	1.94	476.4	5.7
LGC1-1-15	77170	12268	77170	12268	2.94	0.0989	9	310	1.8	580	3.2	96.3	3.29	476.4	5.7
LGC1-1-16	78061	11724	78061	11724	2.82	0.0714	13	320	2.1	600	4.2	104	2.73	476.4	5.7
LGC1-1-17	77921	11865	77921	11865	3.18	0.166	12	320	2.2	590	4.2	91.2	4.81	476.4	5.7
LGC1-1-18	77782	12013	77782	12013	3.39	0.195	11	310	2	580	3.3	84.3	4.88	476.4	5.7
LGC1-1-19	77799	12161	77799	12161	3.57	0.248	10	310	2.6	590	4.6	80.5	5.63	476.4	5.7
LGC1-1-20	78126	11893	78126	11893	3.9	0.311	9	330	2.3	610	5	76.8	6.13	476.4	5.7
LGC1-1-21	77959	12067	77959	12067	3.27	0.148	10	320	2.1	590	3.9	89.6	4.1	476.4	5.7
LGC1-1-22	77902	12243	77902	12243	3.66	0.218	9.4	320	2	590	4.1	79.5	4.77	476.4	5.7
LGC1-1-23	77777	12363	77777	12363	3.6	0.147	8.6	320	2	580	3.2	80.7	3.32	476.4	5.7
LGC1-1-24	77631	12419	77631	12419	3.62	0.231	8.7	320	1.9	590	3.3	80.1	5.13	476.4	5.7
LGC1-1-25	77490	12444	77490	12444	3.39	0.181	8.9	320	1.8	580	3.5	85.5	4.6	476.4	5.7
GJ1-1-A	77744	14021													
GJ1-1-B	76830	13858													
GJ1-1-C	78323	13183													

	x	y	x'	y'	^{4}He/^{3}He	s[^{4}He/^{3}He]	^{3}He	U	s[U]	Th	s[Th]	κ	s[κ]	t	s[t]
GJ1-1-1	77479	13545	77582	12112	1.94	0.0731	17	270	2.4	6.3	0.059	86.9	0.871	460	18
GJ1-1-2	77623	13469	77416	12185	1.8	0.0218	17	270	2.5	6.3	0.072	87.3	1.04	430	8
GJ1-1-3	77642	13623	77537	12309	2.1	0.0955	15	270	2.5	6.1	0.06	82.6	1.19	480	22
GJ1-1-4	77797	13561	77375	12402	1.86	0.0854	20	270	3.1	6.2	0.066	82.5	1.38	420	20
GJ1-1-5	77946	13469	77190	12468	1.86	0.0647	20	270	3.9	6.3	0.079	83.3	1.7	420	17
GJ1-1-6	78087	13344	76982	12504	1.93	0.0951	19	280	2.5	6.3	0.069	85.2	2.19	430	23
GJ1-1-7	76672	13227	77866	11182	1.7	0.0831	14	270	1.9	6.4	0.047	106	4.3	490	30
GJ1-1-8	76852	13271	77779	11371	1.64	0.03	11	280	2.2	6.4	0.053	103	3.55	450	17
GJ1-1-9	76993	13289	77697	11506	1.88	0.111	12	280	1.8	6.4	0.048	100	3.05	510	32
GJ1-1-10	77133	13298	77606	11636	1.81	0.0696	13	280	2.2	6.4	0.057	98.4	2.63	470	21
GJ1-1-11	77333	13321	77487	11827	1.76	0.0962	13	270	2.3	6.4	0.064	95.2	2.05	470	26
GJ1-1-12	77462	13333	77408	11949	1.86	0.086	10	280	2.6	6.5	0.067	93.3	1.76	460	22
GJ1-1-13	77600	13331	77310	12069	1.88	0.102	12	290	2.5	6.7	0.07	91.6	1.65	450	25
GJ1-1-14	76686	13451	78053	11351	1.95	0.137	9.9	270	2.2	6.2	0.048	99.5	3.26	530	39
GJ1-1-15	76863	13464	77940	11515	1.79	0.107	10	280	2.1	6.3	0.05	96.9	2.64	470	29
GJ1-1-16	77063	13515	77846	11726	2	0.107	8.8	280	2.5	6.5	0.052	93	1.83	500	27
GJ1-1-17	77201	13556	77786	11875	2.06	0.0792	8.3	280	2.5	6.6	0.056	90.1	1.33	490	20
GJ1-1-18	76731	13596	78149	11491	1.88	0.182	8.7	280	1.9	6.3	0.051	94.7	2.7	480	46
GJ1-1-19	76863	13630	78086	11630	1.86	0.0807	8.7	280	2.2	6.3	0.059	92.1	2.23	460	22
GJ1-1-20	76987	13656	78023	11757	2.05	0.169	7.8	280	2.2	6.5	0.055	89.8	1.85	490	40
GJ1-1-21	77139	13709	77964	11928	2.08	0.125	7.3	280	2.6	6.3	0.07	86.4	1.55	480	29
GJ1-1-22	77299	13731	77871	12083	2.11	0.192	4.4	270	2.3	6.2	0.054	83.8	1.42	480	43
GJ1-1-23	77468	13746	77767	12242	2.13	0.216	5.8	270	2.4	6.2	0.054	81.2	1.53	470	46

Table 2. Analytical results for the second pair of LGC-1 and GJ-1 shards. Row and column names follow the same convention as Table 1. The large uncertainties of the κ-calibration constant of the sample are caused by the arrangement of the laser spots in two poorly aligned 1D arrays. These uncertainties have been omitted from the error propagation.

	x	y	x'	y'	^{4}He/^{3}He	s[^{4}He/^{3}He]	^{3}He	U	s[U]	Th	s[Th]	κ	s[κ]	t	s[t]
LGC1-2-A	83616	13266													
LGC1-2-B	83949	13588													
LGC1-2-C	83511	14479													
LGC1-2-D	82563	15181													
LGC1-2-3	83547	13646	83547	13646	4.1	0.118	12	310	1.8	590	3.2	69.3	(2.04)	476.4	5.7
LGC1-2-4	83489	13744	83489	13744	4.41	0.254	21	300	2.1	570	3.6	62.5	(3.62)	476.4	5.7
LGC1-2-5	83427	13835	83427	13835	3.91	0.166	14	300	2	580	3.5	71.1	(3.05)	476.4	5.7
LGC1-2-6	83401	13950	83401	13950	4.36	0.16	11	310	1.8	590	3.3	64.7	(2.41)	476.4	5.7

	x	y	x'	y'	$^4\mathrm{He}/^3\mathrm{He}$	s[^{4}He/^{3}He]	^{3}He	U	s[U]	Th	s[Th]	κ	s[κ]	t	s[t]
LGC1-2-7	83322	14035	83322	14035	4.63	0.162	9.6	300	2.6	580	5	60.3	(2.17)	476.4	5.7
LGC1-2-8	83276	14121	83276	14121	4.27	0.15	8.6	310	2.3	580	4.7	65.7	(2.37)	476.4	5.7
GJ1-2-A	83479	15581													
GJ1-2-B	83617	15974													
GJ1-2-C	84275	15383													
GJ1-2-D	84485	14460													
GJ1-2-1	83746	15498	83507	13803	2.28	0.0785	20	230	2.4	5.8	0.057	65.3	(8.01)	480	16
GJ1-2-2	83850	15407	83436	13966	2.42	0.0725	19	230	2.7	5.8	0.069	62.7	(11.2)	480	15
GJ1-2-3	83939	15324	83369	14107	2.67	0.032	7.6	240	2.1	5.9	0.048	60.6	(13.4)	500	7.1
GJ1-2-4	84062	15311	83401	14264	2.56	0.119	8.6	250	2.3	6.1	0.053	55.1	(32.8)	420	19
GJ1-2-5	84102	15218	83302	14349	2.67	0.317	9.4	250	2.3	6.1	0.064	55.5	(24.7)	440	50
GJ1-2-6	84151	15103	83180	14455	2.7	0.106	9	250	2.2	6.1	0.048	56.1	(15.4)	440	17

Table 3. Conventional U–Th–He data for GJ-1 zircon.

aliquot	U [pmol]	Th [pmol]	He [pmol]	t [Ma]	s[t]
1	6.550	0.437	4.105	461.0	19.0
2	24.057	0.980	14.709	449.8	18.0
3	22.283	0.922	13.626	449.8	18.0
4	11.028	0.822	6.839	452.8	18.1
5	6.934	0.197	4.356	462.9	18.0
6	2.940	0.069	1.856	465.5	19.0
7	6.028	0.132	3.752	459.4	19.0
8	2.799	0.042	1.696	448.3	18.2

5 Discussion

The experiments reported in this paper are, in several ways, a best case scenario. They compared two zircon megacrysts of
150 similar age that are compositionally homogeneous. In fact, GJ-1 is so well behaved that it could also be used as a reference material for in-situ U-Th-He dating. It remains to be seen if the method is equally successful when applied to more representative exmples, in which zircons are small and compositionally zoned.

The κ-calibration method hinges on the availability of these well characterised reference materials. They need to be available in sufficient quantities to be included with every proton irradiation. In this regard the method is similar to the $^{40}\mathrm{Ar}/^{39}\mathrm{Ar}$ method.
155 In this study, we have used LGC-1 as a reference material. However, the supply of this standard is limited. As mentioned in

the previous paragraph, GJ-1 is also suitable as a reference material. Unfortunately it, too, is obtained from a single cm-sized crystal. It would be useful to identify a more abundant alternative. Tian et al. (2017) outline a workflow for doing so.

The most important requirement for an age standard is the absence of a distinct diffusion gradient. This, in turn, requires that it has resided at surface conditions for most of its existence after initial rapid cooling. Several Sri Lanka zircons appear to meet
160   this requirement.

The sandwich method requires megacrystic standards, which are large enough to cover the entire sample (Figure 5a). Finer grained standards would need a different analytical design. One option would be to mount the polished sample and standard grains together prior to irradiation, and attach them both to a cover slip made of glass or zirconia (Figure 5b). Assuming that the proton beam intensity varies smoothly within the irradiation stack, the κ-calibration constant could then be obtained by
165   interpolation between the different aliquots of the standard.

The in-situ ^{4}He/^{3}He method requires a sector field noble gas mass spectrometer, unlike the quadrupole instruments that dominate the field of U-Th-He thermochronology today. Combined with the need for proton irradiation, this makes the new method more expensive than the conventional approch. Nevertheless, we would argue that our approach merits further inverstigation, because it opens the door to several new avenues of research.

170   For example, by repeatedly alternating ^{4}He/^{3}He and U, Th measurements in a raster pattern on the same grain, it would be possible to create U-Th-He depth profiles, or even reconstruct a 3-dimensional U-Th-He image by ablating a way the entire crystal, one layer at a time. This would allow the reconstruction of diffusion profiles and thermal history models equivalent to those obtained by ^{4}He/^{3}He step-heating experiments (Tripathy-Lang et al., 2015), but without the need to assume compositional homogeneity.
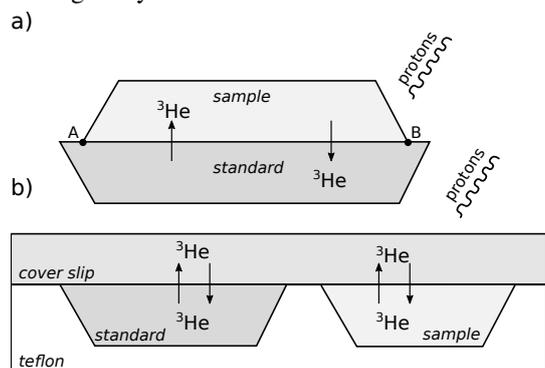
Figure 5. Two ways to quantify and correct proton gradients: a) the sample-standard 'sandwich' method used in this work, where A and B are fiducial points; and b) mounting the sample and the standard in teflon and attaching them to a cover slip made of glass or zirconia. In both designs, the irradiation geometry is fixed so that it is possible to quantify proton flux gradients, and ejection of spallogenic ^{3}He is balanced by injection from neigbouring sources.

6 Conclusions

This paper introduced a novel method for in-situ U-Th-He geochronology that removes the need for absolute U, Th or He abundance measurements. The new method is similar to the ^{40}Ar/^{39}Ar method in two ways. First, it co-irradiates samples with reference materials ('standards') of known age. Second, it connects the sample to the standard using a calibration constant (J for ^{40}Ar/^{39}Ar, κ for in-situ U-Th-^{4}He/^{3}He.

However, the analogy between ^{40}Ar/^{39}Ar and U-Th-^{4}He/^{3}He dating is not perfect. Whereas neutron-induced ^{39}Ar serves as a proxy for the parent nuclide (^{40}K), proton-induced ^{3}He serves as a proxy for ablation pit volume. Therefore, unlike the ^{40}Ar/^{39}Ar method, in-situ U-Th-^{4}He/^{3}He dating still requires the parent(s) and daughter to be measured separately. Although the measurements presented in this paper used U and Th concentrations in ppm, the U-Th-^{4}He/^{3}He method also works with unprocessed U/Si and Th/Si measurements.

The results of the pilot experiment demonstrate that the new approach to in-situ U-Th-He dating produces accurate results. However, further improvements are possible and, indeed, necessary. For example, a new generation of split flight tube noble gas mass spectrometers that are optimised for ^{4}He/^{3}He measurements could significantly increase precision and sensitivity (e.g., Brennan et al., 2020). Similar or even greater gains could be made by improving the proton-irradiation protocol so that more atoms of proton-induced ^{3}He are created per unit volume of zircon (van der Beek et al., 2022). Together these improvements would allow a reduction in laser ablation spot size, which would create a proportional improvement in spatial resolution. Tweaking the proton irradiation protocol may also reduce the strength of the ^{3}He concentration gradient. That, in turn, would simplify the analytical method and bring in-situ U-Th-^{4}He/^{3}He dating closer to practical usability.

Author contributions. PV invented the method, processed the data and wrote the paper; YT and JS carried out the helium measurements; YB carried out the U- and Th-measurements.

Competing interests. PV is an Associate Editor of Geochronology

Acknowledgements. The idea to replace the ^{29}Si 'drill rate proxy' of Vermeesch et al. (2012) by proton-induced ^{3}He was born during one of several fruitful in-situ geochronology discussions with Jeremy Boyce. We would like to thank Ken Farley and Floran Hofmann (Caltech) for arranging the proton-irradiations. This research was funded by NERC grant #NE/K003232/1 and ERC Starting Grant #259504 awarded to PV.

References

Boyce, J. W., Hodges, K. V., Olszewski, W. J., Jercinovic, M. J., Carpenter, B. D., and Reiners, P. W.: Laser microprobe (U-Th)/He geochronology, Geochimica et Cosmochimica Acta, 70, 3031–3039, https://doi.org/10.1016/j.gca.2006.03.019, 2006.

Boyce, J. W., Hodges, K. V., King, D., Crowley, J. L., Jercinovic, M., Chatterjee, N., Bowring, S. A., and Searle, M.: Improved confidence in (U-Th)/He thermochronology using the laser microprobe: An example from a Pleistocene leucogranite, Nanga Parbat, Pakistan, Geochemistry, Geophysics, Geosystems, 10, https://doi.org/10.1029/2009GC002497, 2009.

Brennan, C. J., Stockli, D. F., and Patterson, D. B.: Zircon ^{4}He/^{3}He fractional loss step-heating and characterization of parent nuclide distribution, Chemical Geology, 549, 119 692, 2020.

Danišík, M., McInnes, B. I., Kirkland, C. L., McDonald, B. J., Evans, N. J., and Becker, T.: Seeing is believing: Visualization of He distribution in zircon and implications for thermal history reconstruction on single crystals, Science advances, 3, e1601 121, 2017.

Evans, N., McInnes, B., McDonald, B., Danišík, M., Becker, T., Vermeesch, P., Shelley, M., Marillo-Sialer, E., and Patterson, D.: An in situ technique for (U–Th–Sm)/He and U–Pb double dating, Journal of Analytical Atomic Spectrometry, 30, 1636–1645, 2015.

Farley, K. A., Wolf, R. A., and Silver, L. T.: The effects of long alpha-stopping distances on (U-Th)/He ages, Geochimica et Cosmochimica Acta, 60, 4223–4229, https://doi.org/10.1016/S0016-7037(96)00193-7, 1996.

House, M. A., Farley, K. A., and Stockli, D.: Helium chronometry of apatite and titanite using Nd-YAG laser heating, Earth and Planetary Science Letters, 183, 365–368, https://doi.org/10.1016/S0012-821X(00)00286-7, 2000.

Hurford, A. J. and Green, P. F.: The zeta age calibration of fission-track dating, Chemical Geology, 41, 285 – 317, https://doi.org/10.1016/S0009-2541(83)80026-6, 1983.

Jackson, S. E., Pearson, N. J., Griffin, W. L., and Belousova, E. A.: The application of laser ablation-inductively coupled plasma-mass spectrometry to in situ U–Pb zircon geochronology, Chemical Geology, 211, 47–69, https://doi.org/10.1016/j.chemgeo.2004.06.017, 2004.

Ketcham, R. A., Gautheron, C., and Tassan-Got, L.: Accounting for long alpha-particle stopping distances in (U–Th–Sm)/He geochronology: refinement of the baseline case, Geochimica et Cosmochimica Acta, 75, 7779–7791, 2011.

Kuiper, K. F., Deino, A., Hilgen, F. J., Krijgsman, W., Renne, P. R., and Wijbrans, J. R.: Synchronizing Rock Clocks of Earth History, Science, 320, 500–504, https://doi.org/10.1126/science.1154339, 2008.

Merrihue, C. and Turner, G.: Potassium-argon dating by activation with fast neutrons, Journal of Geophysical Research, 71, 2852–2857, 1966.

Schwanethal, J.: Minimising ^{12}C^{3+} interference on ^{4}He$^+$ measurements in a noble gas mass spectrometer, Journal of Analytical Atomic Spectrometry, 30, 1400–1404, 2015.

Shuster, D. L., Farley, K. A., Sisterson, J. M., and Burnett, D. S.: Quantifying the diffusion kinetics and spatial distributions of radiogenic ^{4}He in minerals containing proton-induced ^{3}He, Earth and Planetary Science Letters, 217, 19–32, https://doi.org/10.1016/S0012-821X(03)00594-6, 2004.

Tian, Y., Vermeesch, P., Danišík, M., Condon, D. J., Chen, W., Kohn, B., Schwanethal, J., and Rittner, M.: LGC-1: A zircon reference material for in-situ (U-Th)/He dating, Chemical Geology, 2017.

Tripathy-Lang, A., Hodges, K. V., Monteleone, B. D., and Soest, M. C.: Laser (U-Th)/He thermochronology of detrital zircons as a tool for studying surface processes in modern catchments, Journal of Geophysical Research: Earth Surface, 118, 1333–1341, 2013.

Tripathy-Lang, A., Fox, M., and Shuster, D. L.: Zircon ^{4}He/^{3}He thermochronometry, Geochimica et Cosmochimica Acta, 166, 1–14, 2015.

van der Beek, P., Denker, A., Amalberti, J., Dittwald, A., Bundesmann, J., and Bernard, M.: Improving the efficiency of proton irradiations for ^{4}He/^{3}He thermochronology, AGU Fall Meeting Abstracts, pp. EP22E–1381, 2022.

Vermeesch, P.: Three new ways to calculate average (U-Th)/He ages, Chemical Geology, 249, 339–347, 2008.

240   Vermeesch, P.: HelioPlot, and the treatment of overdispersed (U-Th-Sm)/He data, Chemical Geology, 271, 108 – 111, https://doi.org/10.1016/j.chemgeo.2010.01.002, 2010.

Vermeesch, P., Sherlock, S. C., Roberts, N. M. W., and Carter, A.: A simple method for in-situ U-Th-He dating, Geochimica et Cosmochimica Acta, 79, 140–147, https://doi.org/10.1016/j.gca.2011.11.042, 2012.